Magnetoacoustic Study of the Rhenium Fermi Surface

L. R. TESTARDI AND R. R. SODEN
Bell Telephone Laboratories, Murray Hill, New Jersey
(Received 3 February 1967)

The magnetic field dependence of the attenuation of longitudinal sound waves with frequencies up to 1 kMc/sec has been studied in very pure rhenium. Ordinary (transverse-field) dimensional resonances, open-orbit resonances, ordinary and giant Landau-level oscillations, longitudinal-field resonances, and cyclotron resonances were observed. Much of the data are consistent with only slight modifications to the 5th- through 8th-zone Fermi-surface sheets calculated by Mattheiss. The dominant signal in the dimensional-resonance data, which yields an isotropic caliper of 0.121 $Å^{-1}$ in the basal plane, probably results from the Γ-centered cavity of the 8th-zone electron sheet. A Landau-level period is observed whose corresponding area is that included by the isotropic caliper. Effective masses obtained from giant Landau-level oscillations and acoustic cyclotron resonance are in reasonable agreement with existing data. The longitudinal-field resonances yield values of the extremal and elliptic limiting point values of $\partial A/\partial k_z$, where A is the cross-sectional area of the Fermi surface in the plane normal to $\mathbf{k}_z$.

I. INTRODUCTION

THE topology and size of the rhenium Fermi surface have recently been studied by galvanomagnetic,[1,2] de Haas–van Alphen[3–5] (dH-vA), and magnetoacoustic experiments.[6,7] In this paper we report and analyze more extensive magnetoacoustic data. The very high purity of our samples allowed the detection of the numerous classical and quantum-field periodic phenomena which can be observed in the attenuation of high-frequency sound. Such data can provide information on the caliper sizes and extremal areas of the Fermi surface, as well as cyclotron masses, Fermi velocities, open-orbit directions and mean free paths. Much of this information, however, is available only for certain orbits or points in k space, and all of the above parameters cannot always be obtained separately.

Following the experimental details which are discussed in Sec. II, the sound velocity, transverse-field dimensional resonances and open-orbit dimensional resonances are discussed in Secs. III, IV, and V, respectively. In Secs. VI, VII, and VIII are discussed the ordinary and giant Landau-level oscillations, cyclotron resonance, and the longitudinal-field resonances. These results are compared, in turn, with the relativistic augmented-plane-wave (APW) calculations of Mattheiss[8] and the existing experimental data referenced above.

II. EXPERIMENTAL

The crystals were prepared by a floating zone-refinement of high-purity rhenium powder. The details of this process have been described elsewhere.[9] Two crystals were grown and prepared for ultrasonic propagation in the three principal directions of this hexagonal crystal. One sample, with a resistance ratio $R(300°K)/R(4.2°K)=22\,000$, was used for propagation along $[1\bar{2}10]$. The other sample, whose resistance ratio was in excess of 55 000, was used for propagation along [0001] and $[10\bar{1}0]$.

Pulse echo measurements of sound attenuation were made with longitudinal waves at frequencies between 200 and 960 Mc/sec. 20 Mc/sec fundamental frequency tourmaline transducers were bonded to the sample with ethyl alcohol and driven at the overtone operating frequencies by a pulse rf generator. Gating and integrating a detected echo allowed continuous recording of the sound attenuation. For a study of the transverse-field dimensional resonances, field-derivative methods were used with phase-sensitive detection of the field-modulated echo amplitude. The high electrical conductivity of these crystals required low modulation frequencies (2–4 cps) to achieve adequate field penetration of the sample. Since the rf pulse repetition rate (~5 kc/sec) was much larger than the field modulation rate, no modification of standard pulse operating methods was required.

For studies in the longitudinal-field configuration, field strengths up to 100 kG were used without modulation.

Measurements of 20-Mc/sec longitudinal-wave velocities along the three crystallographic directions were made with the McSkimin pulse-superposition method.[10] These data are necessary for the analysis of the dimensional resonances.

III. SOUND VELOCITY

The results of the sound velocity measurements are given in Table I. The thermal-expansion correction, $l(300°K)/l(T°K)-1$ is not known but can be estimated

[1] N. E. Alekseevskii, V. S. Egorov, and B. N. Kazak, Zh. Eksperim. i Teor. Fiz. 44, 1116 (1963) [English transl.: Soviet Phys.—JETP 17, 752 (1963)].
[2] W. A. Reed, E. Fawcett, and R. R. Soden, Phys. Rev. 139, A1557 (1965).
[3] A. C. Thorsen and T. G. Berlincourt, Phys. Rev. Letters 7, 244 (1961).
A. S. Joseph and A. C. Thorsen, Phys. Rev. 133, A1546 (1964).
[5] A. C. Thorsen, A. S. Joseph, and L. E. Valby, Phys. Rev. 150, 523 (1966).
[6] C. K. Jones and J. A. Rayne, Phys. Letters 14, 13 (1965).
[7] C. K. Jones and J. A. Rayne, Phys. Rev. 139, A1876 (1965).
[8] L. F. Mattheiss, Phys. Rev. 151, 450 (1966).
[9] R. R. Soden, G. F. Brennert, and E. Buehler, J. Electrochem. Soc. 112, 77 (1965).
[10] H. J. McSkimin, J. Acoust. Soc. Am. 33, 12 (1961).

TABLE I. 20-Mc/sec longitudinal wave sound velocities.

Direction	Velocity$\times\frac{l(300°K)^a}{l(T)}$[$10^5$ cm/sec]		
	300°K	78°K	4.2°K
[0001]	5.705	5.821	5.835
[10$\bar{1}$0]	5.421	5.517	5.528
[1$\bar{2}$10]	5.421	5.517	5.528

[a] l is the length of the crystal.

to be $\sim 0.2\%$ at the lower temperatures. The hexagonal symmetry requires that the [10$\bar{1}$0] and [1$\bar{2}$10] velocities be equal. The measured values show the good agreement obtained between the two crystals. The experimental error in these measurements was estimated to be $\sim 0.1\%$.

IV. TRANSVERSE-FIELD DIMENSIONAL RESONANCES

The attenuation of sound propagating normal to an applied magnetic field exhibits an oscillatory field dependence which arises from the dimensional matching of the electron orbit size to an integral number of sound wavelengths $n\lambda$.[11] The relation between the field period $\Delta(1/H)$ and the k-space caliper radius k_c is

$$k_c=\frac{e\lambda}{2\hbar c\Delta(1/H)}. \tag{1}$$

The conditions necessary to observe this effect are that (i) the cyclotron frequency $\omega_c=eH/m^*c$ be greater than the scattering frequency τ^{-1}, and (ii) the electron mean free path l be greater than $\lambda/2\pi=q^{-1}$.

In Eq. (1) k_c is the caliper size of the Fermi surface in a direction normal to **H** and **q**. For **q** normal to a mirror symmetry plane of a given Fermi-surface sheet, the caliper dimensions are the diameters of that sheet in the direction of **q**×**H**.

The Fermi surface of rhenium has recently been obtained from relativistic (APW) calculations by Mattheiss.[8] In Fig. 1 the calculated Fermi-surface contours in an unfolded 1/24 Brillouin-zone section are shown. The 5th- (ellipsoid), 6th- ("dumbbell"), and 7th-zone hole surfaces, all centered at the point L, are shown in Figs. 2 and 3. Most of the electrons are contained in an 8th-zone piece of approximately cylindrical shape (see Fig. 3) which contacts the {0001} zone boundaries. A small cavity, centered at Γ, exists within this piece. A 9th-zone electron piece also exists but its shape has not been obtained accurately from the calculations.

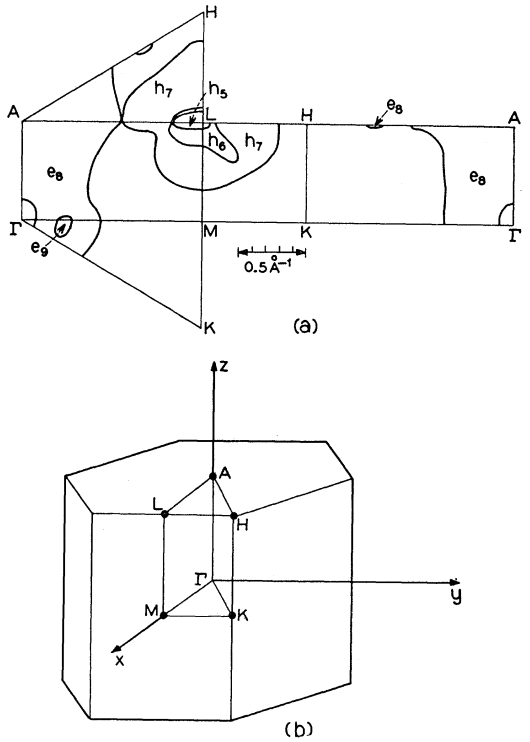

FIG. 1. (a) Rhenium Fermi-surface contours in an unfolded 1/24 Brillouin-zone section. The labeling denotes electrons or holes and the zone number. (b) The Brillouin zone for the hexagonal structure.

A. $\mathbf{q}_L\|[0001]$

The strongest set of oscillations is obtained with the sound propagating along the hexagonal axis. A partial trace of the data obtained at 960 Mc/sec is shown in Fig. 4. Oscillations could be detected at fields as low as 30 G. The amplitude of the oscillations increased on cooling from 4.2 to 1.7°K indicating that a thermal contribution to the resistivity is detectable at 4.2°K for this sample. The oscillations shown in Fig. 4(a) have periods $\Delta(1/H)=3.70\times10^{-4}$ and 3.89×10^{4} G^{-1} which, to within $\frac{1}{2}\%$, are independent of field direction in the basal plane. (The amplitude is also isotropic although this is determined with less precision.) With the sound velocity given in Table I these periods correspond to caliper radii 0.124 and 0.118 Å^{-1}. The estimated error is 1%.

In the usual physical picture of the dimensional resonance the cyclotron motion of the electron is calipered by a spatially adiabatic sound wave, i.e., $\omega_c\gg\omega$. If $m^*/m>1/15$ the cyclotron resonance condition $\omega_c=\omega$ at 960 Mc/sec will occur at fields above 30 G where, since oscillations occur, $\omega_c\tau>1$. Gavenda and Chang[12] have shown that when dimensional-resonance oscillations are observed in the field ranges of cyclotron resonance a beat pattern occurs with the null and phase reversal occurring at $\omega/\omega_c=n/2$ (n an odd interger). (Physically the effect arises from the change in the

[11] M. H. Cohen, M. J. Harrison, and W. A. Harrison, Phys. Rev. 117, 937 (1960).

[12] J. D. Gavenda and F. H. S. Chang, Phys. Rev. Letters 16, 228 (1966).

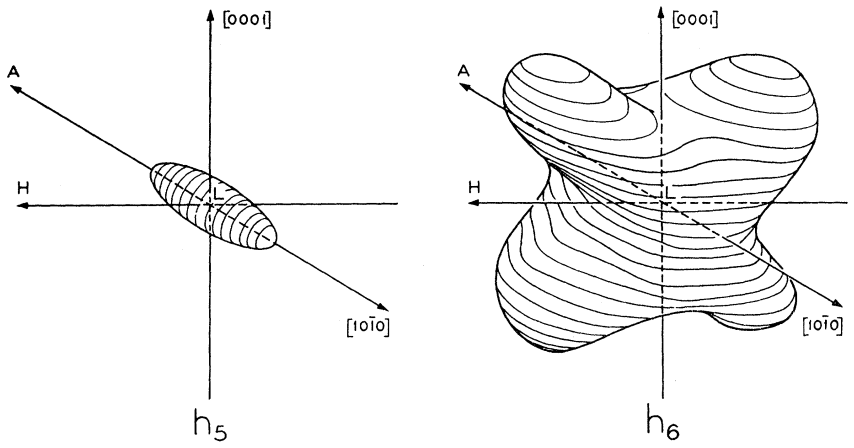

FIG. 2. The 5th- and 6th-zone hole sheets; h_5 is situated within h_6 and contact occurs along [10$\bar{1}$0].

relative phase of the orbit motion and sound wave at these fields.) With this interpretation the data shown in Fig. 4 yield $\Delta(1/H)=3.79\times10^{-4}$ G^{-1} and $m^*/m=0.39\pm0.02$.

The corresponding radial caliper dimension, 0.121 Å^{-1}, which is isotropic in the basal plane would imply a Fermi-surface sheet with circular cross section in the basal plane of area 0.046 ± 0.001 Å^{-2}. From dH-vA studies Joseph and Thorsen[4] report a basal plane extremal area of 0.0434 Å^{-2} which, from the anisotropy behavior, is associated with the ellipsoids h_5. However, our data show neither the size anisotropy (a 3.5/1 principal-axis ratio in the basal plane) nor the three-period-beat anisotropy expected from these pieces. With $\mathbf{H}\perp[0001]$ weak oscillations are sometimes observed to interfere with the dominant period in the field range 30–150 G. These periods, which are anisotropic in the basal plane, correspond to caliper sizes ~0.06–0.15 Å^{-1} and probably arise from h_5.

The failure to see a dH-vA period corresponding to the isotropic basal-plane caliper may indicate that the sheet is reentrant, e.g., torus-shaped. (Such a shape occurs for e_8 if the Fermi level used for Fig. 1 is raised by ~0.07 eV.)[8] Under such circumstances interchanging the directions of $\mathbf{q}$ and $\mathbf{H}$ will not yield the same caliper size. With $\mathbf{H}\|[0001]$ caliper sizes of approximately 0.12 Å^{-1} are found along [10$\bar{1}$0] and [1$\bar{2}$10] (see below). However, the reduced accuracy of this data cannot provide an unequivocal identification.

The calculations of Mattheiss show two segments of the Fermi surface which might be responsible for the isotropic period. These are the Γ-centered cavity of e_8, not identified in the dH-vA data, and the piece e_9 which may have a toroidal form. Thorsen, Joseph, and Valby[5]

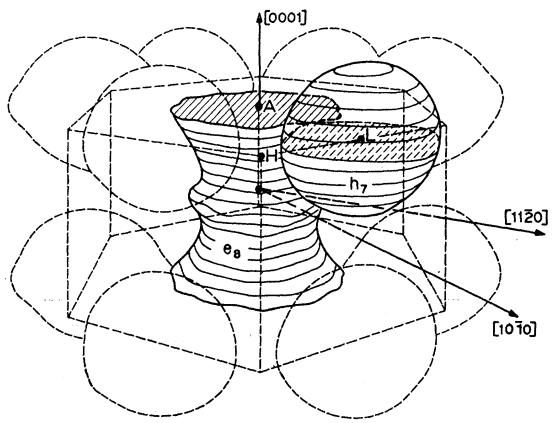

FIG. 3. The 7th-zone hole and 8th-zone electron sheets; h_5 and h_6 are located within h_7 which contacts e_8 along [10$\bar{1}$0].

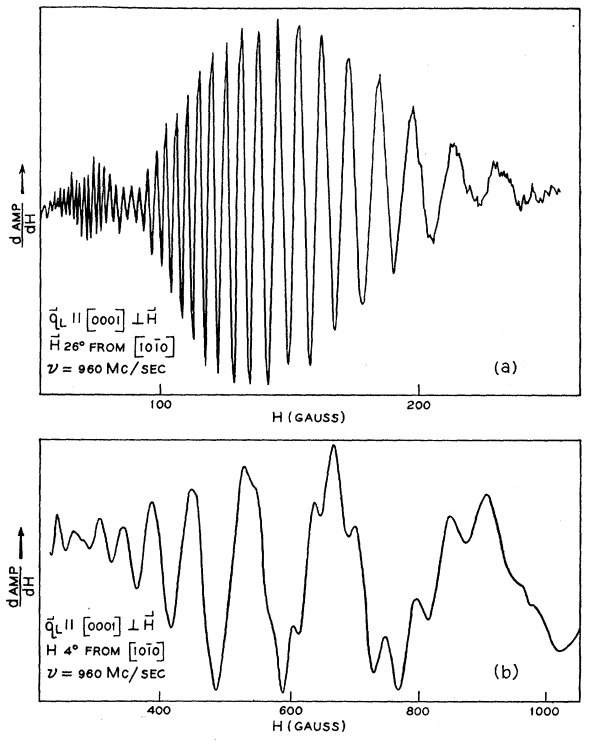

FIG. 4. Field derivative of echo amplitude versus magnetic field for $\mathbf{q}\|[0001]\perp\mathbf{H}$ and $\nu=960$ Mc/sec. (a) H 26° from [10$\bar{1}$0]. 0–250 G. (b) H 4° from [10$\bar{1}$0]. 0–1000G.

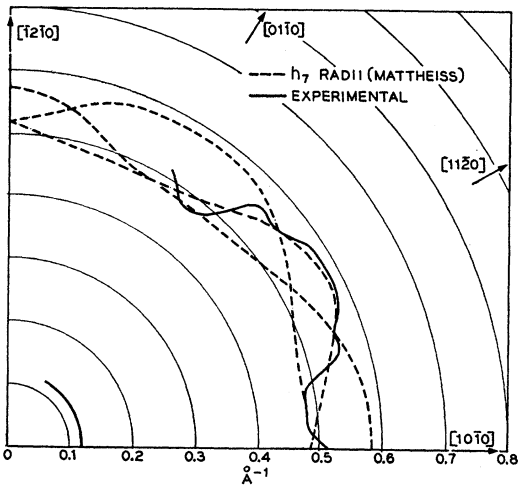

FIG. 5. Observed and calculated basal-plane caliper sizes. The experimental data, obtained with $\mathbf{q}\|[0001]$, generally showed beats of 1 in 5 to 1 in 7. The calculated values are the radii for the three inequivalent symmetry-related pieces h_7.

(TJV) have associated part of their dH-vA data and the isotropic caliper dimension with the latter sheet assumed to be formed by six balls (responsible for all isotropic periods) connected by short necks. However, neither the dH-vA results nor our data (taken at 2° intervals in the basal plane) indicate the existence of necks. The size and shape of the e_8 cavity and e_9 have not been obtained accurately in the APW calculations. Additonal magnetoacoustic data believed to be associated with one (or both) of these pieces are presented in the following sections.

Above 300 G small period oscillations occur [see Fig. 4(b)]. The angular variation of the caliper size given by these oscillations is shown in Fig. 5. The data, taken at 2° intervals, compare quite well with the radii of h_7 calculated by Mattheiss. (Since $\mathbf{q}$ is normal to a mirror plane of h_7 the experimental data give radii directly.) The symmetry-related pieces (whose diameters are given in Fig. 5) result in the occurrence of beats (1 in 5 to 1 in 7) which were observed throughout the basal plane. The beat pattern, complicated by the strong low-frequency background, could not be analyzed in many cases. The experimental results (Fig. 5) generally pertain to the strongest signal and have a field-period accuracy of $\sim 3\%$. Note that since the basal-plane dimensions are obtained with $\mathbf{H}\perp[0001]$ the orbits being calipered generally will not include the h_7-e_8 breakdown point (see Fig. 3).

B. $\mathbf{q}_L\|[10\bar{1}0]$

Measurements were made at a frequency of 515 Mc/sec. Data for caliper sizes less than 0.25 Å^{-1} are shown in Fig. 6. Throughout the $(10\bar{1}0)$ plane good agreement is obtained with the radii of h_5 (ellipsoids) calculated by Mattheiss and also derived from dH-vA data. (The latter determinations agree to within several percent.) For the symmetry related (60° rotated) ellipsoids no caliper dimensions were obtained within 30° of the basal plane possibly because of the higher effective mass for the orbits involved.

A dimensional contour of size ranging from 0.20 to 0.12 Å^{-1} is also obtained (see Fig. 6). Along [0001] the caliper sizes are in good agreement with the calculated dimensions of h_6. For the sheets of h_6 which do not have a mirror plane normal to $[10\bar{1}0]$ the calipered orbit passes partly over the ears and leads to a maximum (0.192 Å^{-1}) and a minimum (0.165 Å^{-1}) caliper size. However, the experimental agreement with both values is probably accidental. The dH-vA results indicate that the h_6 lobes which extend in a direction midway between [0001] and $[1\bar{2}10]$ present a considerably smaller area for field directions in a $(10\bar{1}0)$ plane than that given by the calculations. It is unlikely that this modification would give rise to the two branches in Fig. 6 which remain well separated for 20° or more from [0001]. The remaining angular data show sizes much smaller than those calculated by Mattheiss or obtained in the dH-vA studies for h_6. (Orbits whose calipers are the radii of h_6 may not be easily observed because they include the h_5-h_6 breakdown points where scattering may reduce the $\omega_c\tau$.) Along $[1\bar{2}10]$ a caliper of 0.122 Å^{-1} is obtained which we associate with the isotropic basal-plane caliper of 0.121 Å^{-1} found with $\mathbf{q}\|[0001]$. This caliper can be tracked to within 40° of [0001] where weak signals and an irregularity in the contour make it difficult to estab-

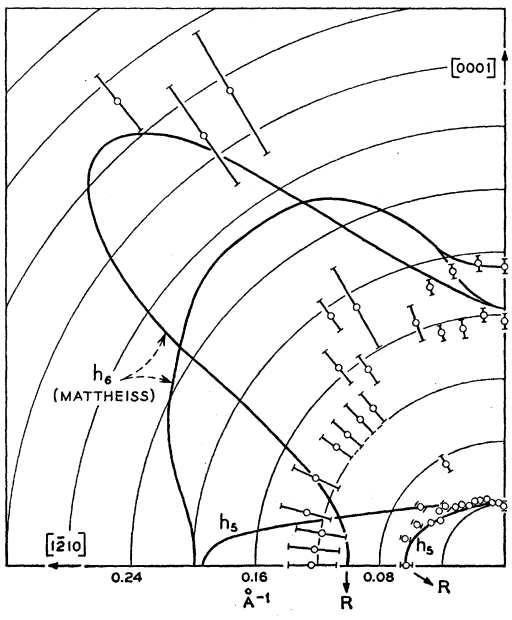

FIG. 6. Observed and calculated caliper sizes less than 0.25 Å^{-1} in the $(10\bar{1}0)$ plane. For calculated values, contours labeled R give radii for sheets where $\mathbf{q}$ is normal to a mirror plane. Unlabeled contours give caliper sizes for inequivalent symmetry related pieces. For h_5 the calculated values were obtained from the data of Joseph and Thorsen.

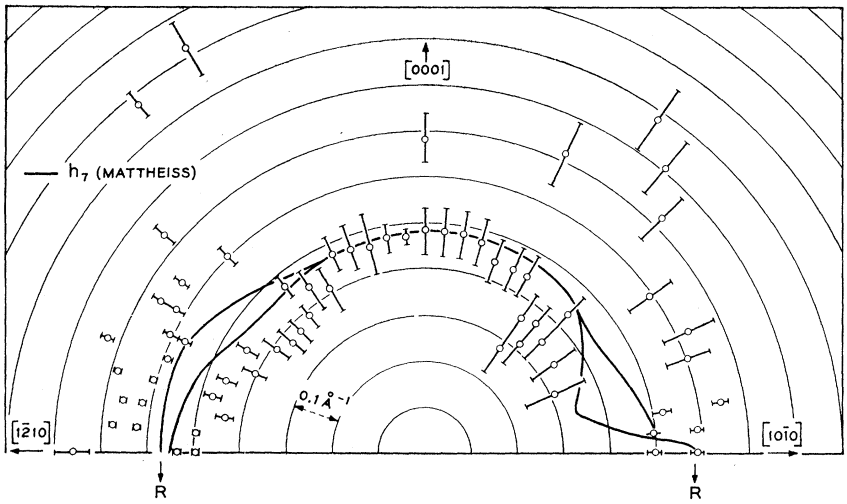

FIG. 7. Observed and calculated caliper sizes between 0.3 and 0.9 Å^{-1} in the (10$\bar{1}$0) and (1$\bar{2}$10) planes. For the calculated values contours labeled R give radii for sheets where $\mathbf{q}$ is normal to a mirror plane. Unlabeled contours give caliper sizes for inequivalent symmetry-related pieces.

lish continuity with the remaining angular data. Assuming continuity with the lower branch near [0001] leads to a contour whose included area is 6×10^{-2} Å^{-2}. Since the oscillations corresponding to the basal plane calipler (0.21 Å^{-1}) are isotropic in amplitude as well as period, we further assume that the contour describes a figure of revolution about [0001]. Such a sheet should have a dH-vA period of approximately 16×10^{-8} G^{-1} for all field directions in the basal plane. The orbit radii and dH-vA period shoud remain roughly constant for field directions up to 20°–35° from the basal plane where a rapid change in orbit size probably occurs which may be responsible for the weak dimensional resonance oscillations. TJV have reported a period (P_7) of 15.2×10^{-8} G^{-1} which is isotropic in the basal plane. This period can be followed out to 35°–40° from the basal plane varying less than 6% in that interval.

For $\mathbf{H}\|[0001]$ the proposed sheet would have a dH-vA period of $20.8\pm0.4\times10^{-8}$ G^{-1} determined from the isotropic caliper obtained with $\mathbf{q}\|[0001]$. From the behavior of the caliper anisotropy (Fig. 6) this period should remain roughly constant for $\mathbf{H}$ within 10° of [0001] beyond which some decrease probably occurs. We show in Sec. VI that Landau-level oscillations with a period $20.8\pm0.3\times10^{-8}$ G^{-1} for $\mathbf{H}\|[0001]$ have been obtained in the ultrasonic attenuation. These oscillations have a second harmonic content comparable to the fundamental and may be those reported by TJV to have the period 10.4×10^{-8} G^{-1}. Although the decrease in the dH-vA period with increasing angle from [0001] is not inconsistent with the errors in the caliper measurements, it is not clear from the proposed sheet why this period can only be tracked for only 10°–20°.

In view of the symmetry of the proposed sheet it is reasonable to associate it with the Γ-centered cavity of e_8. Mattheiss finds the dimensions 0.14 Å^{-1} along [0001] and 0.11 Å^{-1} (isotropic) in the basal plane for a Fermi energy of 0.825 Ry.[13] Although these values cannot be considered accurate, they are in reasonable accord with the corresponding values 0.16 and 0.12 Å^{-1} for our proposed sheet.

Caliper sizes between 0.3 and 0.7 Å^{-1} in the (10$\bar{1}$0) plane are shown in Fig. 7. Those sizes less than 0.54 Å^{-1} agree fairly well with the calipers of the calculated 7th-zone holes. Signals corresponding to these sizes generally showed beats (1 in 4 to 1 in 8) expected for the two h_7 branches, but they usually could not be resolved. The experimental results show the caliper dimensions[14] to have a larger minimum midway between [1$\bar{2}$10] and [0001] than given by the calculations. The area included by the data contour is about 10–15% smaller than the value given by Mattheiss for h_7. This is consistent with the dH-vA results.

Caliper sizes larger than 0.5 Å^{-1} are shown in Fig. 8.

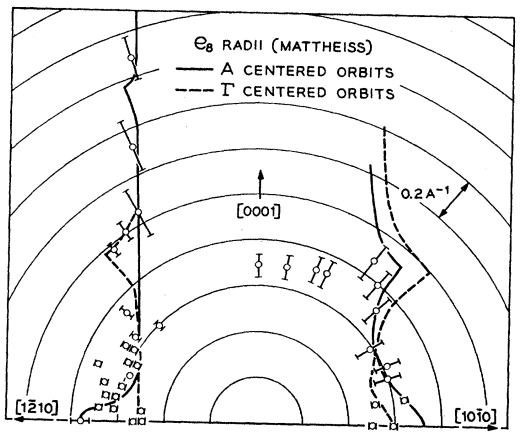

FIG. 8. Observed and calculated caliper sizes larger than 0.5 Å^{-1} in the (10$\bar{1}$0) and (1$\bar{2}$10) planes. Calculated sizes are radii. Some of this data are also given in Fig. 6.

[13] Only these dimensions for the Γ-centered e_8 cavity have been calculated. The spheriodal shape shown in Fig. 1 is representative only.

[14] Since h_7 is roughly spherical, differences between caliper dimensions and radii, when they exist, will be small over much of the surface.

These data provide a good confirmation of the 8th-zone electron cylinder calculated by Mattheiss. The radii of the calculated sheet for A-centered and Γ-centered orbits show discontinuities at those angles where the orbit is abruptly made to pass over the protrusions of e_8 in the ALH plane. At fields less than 3000-G oscillations corresponding to the e_8 caliper can be tracked from $[1\bar{2}10]$ to within 20° of [0001] where the orbit encompasses more than two zones.

Along $[1\bar{2}10]$ the experimental caliper 0.76 Å^{-1} is in excellent agreement with the radius along AH of the top face of e_8 calculated by Mattheiss.

Within 20° of the basal plane the data indicate a small deviation of e_8 from the calculated form. On going from $[1\bar{2}10]$ to [0001], the Γ-centered radius may, within the first 20°, increase beyond and then decrease back to the values for the calculated surface. This modification, which is roughly an inversion of what occurs in the $A\Gamma M$ plane, would tend to eliminate the minimal area in e_8 somewhat above the ΓMK plane. This extremal area has not been found in the dH-vA studies.

C. $\mathbf{q}_L \| [\bar{1}2\bar{1}0]$

Caliper dimensions smaller than 0.12 Å^{-1} are given in Fig. 9. Data in good agreement with h_5 can be followed for 60° from [0001]. Closer to $[10\bar{1}0]$ the increasing effective mass may cause the disappearance of these oscillations. The remaining data do not fit the h_5 or h_6 sheets. The 0.08 Å^{-1} caliper which is continuous and nearly isotropic within 50° of [0001] is not observed in the $(10\bar{1}0)$ plane (see Fig. 6). This size may be associated with e_9.

The 0.12 Å^{-1} caliper obtained within 25° of $[10\bar{1}0]$ is similar to the caliper behavior about $[1\bar{2}10]$. This is consistent with the proposed sheet for the e_8 cavity being a figure of revolution. Because of reduced sample purity and operating frequency the oscillations for this period were weak and could not be tracked over the full quadrant. Jones and Rayne[7] have obtained a 0.18 Å^{-1} caliper within 20° of [0001] in the $(1\bar{2}10)$ plane.

Caliper sizes greater than 0.12 Å^{-1} are given in Fig. 7. Sizes less than 0.5 Å^{-1} are in reasonable agreement with those calculated for h_7. Near [0001] the agreement is excellent. About 35° from [0001] toward $[10\bar{1}0]$ the measured calipers become smaller than the calculated values. This is consistent with the similar constriction in h_7 found in the $(10\bar{1}0)$ plane. The smaller extremal area which would result from this constriction is again in agreement with the dH-vA results. At 65° from [0001] the oscillations attributed to h_7 become very weak and it is not possible to establish continuity with the remaining angular data. The additional caliper of approximately 0.3 Å^{-1} found near 35° from [0001] in the $(1\bar{2}10)$ plane probably pertains to the "ears" of h_6 which came closest to h_7. The experimental value is, to within error, in agreement with the calculated value.

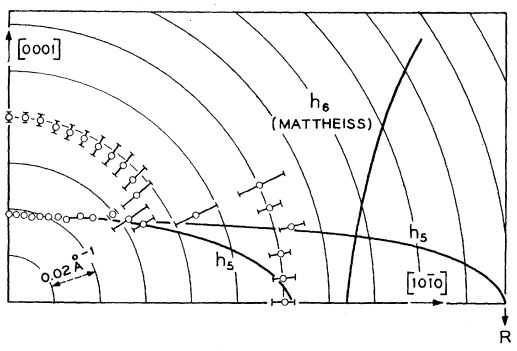

FIG. 9. Observed and calculated caliper sizes smaller than 0.12 Å^{-1} in the $(1\bar{2}10)$ plane. For the calculated values contours labeled R give radii for sheets where $\mathbf{q}$ is normal to a mirror plane. Unlabeled contours give caliper sizes for inequivalent symmetry related pieces. For h_5 the calculated values are obtained from the data of Joseph and Thorsen.

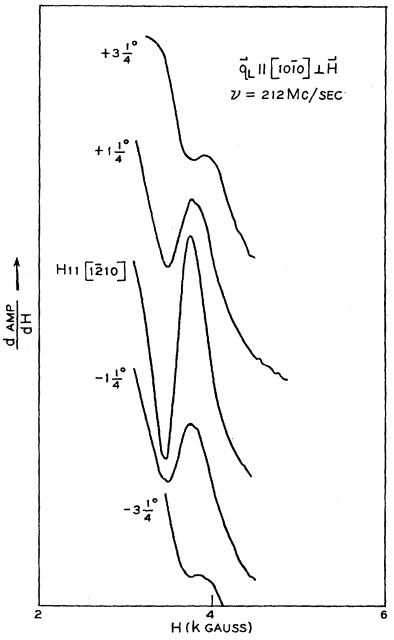

FIG. 10. Field derivative of echo amplitude (inverse absorption) for $\mathbf{q} \| [10\bar{1}0] \perp \mathbf{H}$, and $\gamma = 212$ Mc/sec. The open-orbit resonance signal occurs at 3550 G.

Calipers greater than 0.5 Å^{-1} are replotted in Fig. 8. Good agreement with the radii of e_8 is generally obtained. However the maxima in the radii for both A- and Γ-centered orbits is not evident in the data. In this plane the radii could be calipered to within 35° of [0001] where the orbit extends over somewhat more than one zone. At 25° from [0001] where the orbit encompasses almost two zones, the calipered dimension corresponds to the zone periodicity in that direction rather than the maximum radius of the orbit. The caliper obtained along [0001] is discussed in the next section.

V. OPEN-ORBIT RESONANCE

With $\mathbf{H} \perp [0001]$ open orbits along the cylinder e_8 occur which give rise to dimensional resonances with

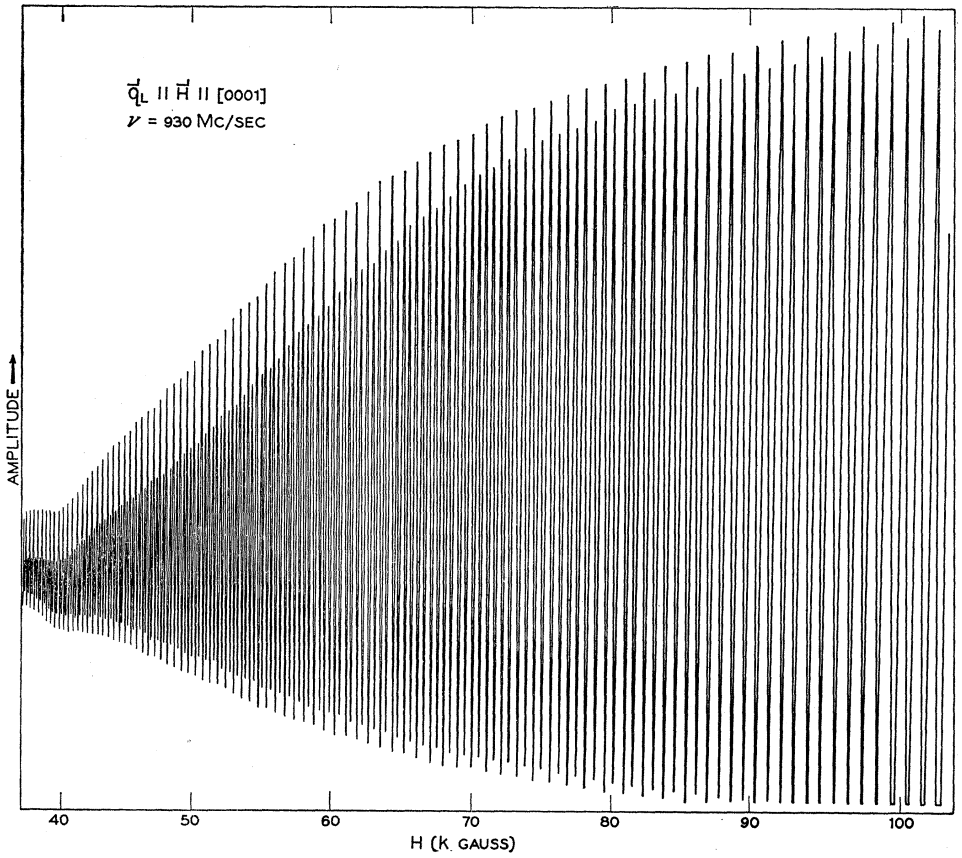

FIG. 11. Landau-level oscillations in the echo amplitude versus magnetic field for $\mathbf{q}\|\mathbf{H}\|[0001]$ and $\nu=930$ Mc/sec and $T=1.3°$K. Some amplitude limiting in the detection system occurs above 60 kG.

the periodicity of the reciprocal lattice in that direction.[15] The fundamental resonant sound absorption due to the open orbit motion with $\mathbf{q}\|[10\bar{1}0]$ and $\mathbf{H}\|[1\bar{2}10]$ is shown in Fig. 10. Resonances at the subharmonics are not seen because of the reduced effective $\omega_c\tau$ and the large interfering signals from ordinary dimensional resonances. With a frequency of 212 Mc/sec the fundamental peak occurs at 3550 G corresponding to a k-space (diam) [0001] periodicity of 1.406 ± 0.01 Å^{-1}. (The phase is zero for open-orbit resonance oscillations.)[15] The zone height, calculated from the room-temperature lattice parameters, is 1.40 Å^{-1}. Thermal contraction should increase this value by several parts per thousand.

The linewidth of the resonance absorption peak, $\Delta H/H$, is equal to the reciprocal ql value.[15] The resonance width shown in Fig. 10 indicates that the mean free path of the open-orbit carrier is about 0.04 mm or roughly two zone lengths in real space at 3.5 kG (effective $\omega_c\tau=2\times2\pi$). This size corresponds to the largest orbits on the e_8 cylinder found in the ordinary dimensional resonances.

For $\mathbf{H}$ slightly tilted from $[1\bar{2}10]$ in the $(10\bar{1}0)$ plane the open-orbit resonance peak is diminished in amplitude and shifts to slightly higher fields. The latter behavior, which is partly due to a lengthing of the tilted-orbit period, is complicated by the large varying background signal. The decrease in signal amplitude within 3° of $[1\bar{2}10]$ is more rapid than one would expect with the comparatively modest ql and $\omega_c\tau$. This may indicate that the e_8-h_7 breakdown point, which should have critical orientation effects, may be important in the strength of the open-orbit resonance amplitude.

For $\mathbf{q}\|[1\bar{2}10]$ and $\mathbf{H}\|[10\bar{1}0]$ and [0001] open-orbit resonance signal (with subharmonics) is also seen. The accuracy of the data was only $\pm10\%$. However, no orbits other than the e_8 open orbits should be of comparable size.

VI. LANDAU-LEVEL OSCILLATIONS

Landau-level (dH-vA type) oscillations of sound absorption in fields to 100 kG were observed with $\mathbf{q}\|\mathbf{H}$ along the three symmetry directions. Data obtained with $\mathbf{H}\|[0001]$ at 930 Mc/sec (shown in Fig. 11) yield a fundamental period $\Delta(1/H)=20.8\pm0.3\times10^{-8}$ G^{-1}. At 100 kG the oscillations have an amplitude of greater than 50 dB/cm which is of the order of the zero-field attenuation resulting from all carriers. The strong second-harmonic signal indicates that the spin splitting of the Landau levels is almost equal to one-half the Landau-level separation. This fundamental period has

[15] E. A. Kaner, V. G. Peschanskii, and I. A. Privorotski, Zh. Eksperim. i Teor. Fiz. **40**, 214 (1961) [English transl.: Soviet Phys.—JETP **13**, 147 (1961)].

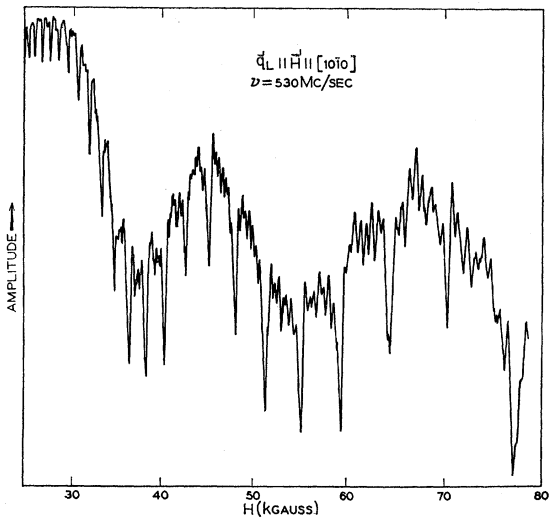

FIG. 12. Giant quantum oscillations of echo amplitude for $\mathbf{q}\|\mathbf{H}\|[10\bar{1}0]$, $\nu=530$ Mc/sec and $T=1.3$°K.

not been reported in the dH-vA studies. Although the [0001] period for the h_5 ellipsoids, 22.0×10^{-8} G^{-1}, is close to what we have found, the discrepancy is outside the combined experimental errors ($\pm0.9\times10^{-8}$ G^{-1}). Furthermore, for **H** within 0.6° of [0001] (our probable orientation accuracy)[16] the ellipsoid period is not observed because of breakdown between h_5 and h_6.[4] Our period is in very good agreement with the period $20.8\pm0.4\times10^{-8}$ G^{-1} expected for the basal-plane isotropic caliper obtained with $\mathbf{q}\|[0001]\perp\mathbf{H}$. This suggests that the sheet responsible for this caliper is simple and closed.[17] At high fields the second-harmonic oscillations become comparable in amplitude with the fundamental. This may be the source of the period 10.4×10^{-8} G^{-1} observed within 10° of [0001] in the high-field dH-vA work. The large amplitudes of both the geometrical and Landau-level oscillations indicate a strong interaction of these carriers with [0001] longitudinal sound.

With $\mathbf{H}\|[10\bar{1}0]$ the "giant" oscillations[18] in sound attenuation shown in Fig. 12 are obtained. The period of these oscillations is 13.1×10^{-7} G^{-1} which is in agreement with the value reported by Joseph and Thorsen for the ellipsoids in the light-mass direction. The attenuation peaks result from electron absorption of the generated phonons with no change in Landau level.[19] The simultaneous conservation of energy and momentum can only occur for certain points on (or very near) the Fermi surface. The spiked attenuation peaks of Fig. 12 occur for field values where the Landau levels pass these allowed points. In order that this process lead to large attenuation ("giant oscillations") the following condition, given by Quinn,[18] must be satisfied:

$$ql>\frac{V_F}{V_S}\left(\frac{2nkT}{m^*V_S^2}\right)^{1/2}. \tag{2}$$

Here n is the Landau-level number, and V_F and V_S are the Fermi and sound velocities. Estimates of the quantities in Eq. (2) indicate that the inequality is approximately satisfied.

If Eq. (2) is well satisfied, the line shape of the giant quantum oscillations can provide information on the cyclotron mass. The relationship, given by Shapira and Lax,[20] between the full width δH at half-amplitude of the attenuation spikes and the cyclotron frequency is

$$\delta H/\Delta H=3.53kT/\hbar\omega_c, \tag{3}$$

where $\Delta H=H^2\Delta(1/H)$ is the spacing between Landau-level oscillations. With the data of Fig. 12 we obtain $m^*/m=0.15\pm0.05$ which is in reasonable agreement with the value 0.12 estimated from dH-vA results.

In addition to the giant quantum oscillations a period of $\sim1.5\times10^{-7}$ G^{-1}, previously reported by TJV[5] is observed with $\mathbf{H}\|[10\bar{1}0]$. This is the period which we have associated with the Γ-centered e_8 cavity.

With $\mathbf{H}\|[1\bar{2}10]$ Landau-level oscillations with periods 11.7, 1.25, and 1.50×10^{-7} G^{-1}, all previously reported,[4,5] have been observed. These oscillations have the normal sinusoidal line shape. The failure to see the giant oscillations in this orientation is due to the larger masses for the orbits involved and to smaller mean free paths in this crystal.

VII. CYCLOTRON RESONANCE

If $\omega_c\tau>1$, cyclotron resonance in the sound absorption can be observed at $\omega=n\omega_c$ with the magnetic field either parallel or normal to the sound propagation vector.[11] For the range of frequencies used in our studies the condition on $\omega_c\tau$ is difficult to satisfy except in very pure materials. (For $\omega=2\pi10^9$ sec^{-1}, $\omega_c=\omega$ at ~330 G for $m^*/m=1$.) In principle the cyclotron (temperal) resonances can be distinquished from the geometrical (dimensional) resonances by using shear and longitudinal waves of the same frequency which have different wavelengths. Unfortunately, for $\mathbf{q}\|[0001]$ we were unable to detect shear-wave echoes in the hundred Mc/sec range. For $\mathbf{q}\perp[0001]$ the difference in the strengths of the oscillations for the two modes led to some uncertainty in the interpretation of the data. The identification of cyclotron resonance in our data is based on the

[16] Larger misorientations would cause beats from inequivalent ellipsoids with all periods being greater than 22.0×10^{-8} G^{-1}. Beats, probably caused by the ellipsoids, do occur in our data for **H** slightly tilted from [0001].

[17] If the surface is toroidal our results indicate that in the basal plane the inside diameter is $\frac{1}{3}$ the outside diameter.

[18] J. J. Quinn, Phys. Rev. **137**, A889 (1965).

[19] Transitions in which the Landau level is changed may occur with longitudinal waves if the Fermi surface is anistropic (see Ref. 18). These transitions can occur only if the Landau-level separation is not too large. The maximum field for this process, given by $\omega/\omega_c>V_S/V_F$ (V_S and V_F are sound and Fermi velocities), is estimated to be less than the lowest field for which oscillations are seen.

[20] Y. Shapira and B. Lax, Phys. Rev. Letters **12**, 166 (1964).

fact they occur in the expected field range while an interpretation based on dimensional resonances would yield linear dimensions of the Fermi surface considerably smaller than the shortest dimension of the ellipsoids.

Cyclotron resonance was observed with $\mathbf{q}_L \| [10\bar{1}0] \perp \mathbf{H}$ and $\mathbf{H}$ near [0001]. Generally only two or three oscillations could be detected over the noise. With $\mathbf{H} \| [0001]$ the observed mass was $m^*/m = 0.45 \pm 0.1$. Away from [0001] the signal amplitude decreases while the mass increases slowly, the increase reaching $\sim 10\%$ at 15° from [0001]. At larger angles no masses could be obtained because of weak beating signals. Our values probably pertain to h_6 for which Joseph and Thorsen report $m^*/m = 0.47$ with $\mathbf{H} \| [0001]$ and which increases by 15% within 15° of [0001]. An additional mass of 0.9 ± 0.1 is also observed within 15° of [0001]. Weak oscillations corresponding to a mass of 1.7 ± 0.3 are found throughout much of the $(10\bar{1}0)$ plane. In view of the approximate isotropy we associate these values with h_7. This is in agreement with the value $m^*/m = 1.9 \pm 0.7$ associated with a period expected for h_7 which has been reported by Thorsen and Berlincourt.[3]

With $\mathbf{q}_L \| [0001] \perp \mathbf{H}$ weak oscillations are observed through much of the basal plane whose periods correspond to $m^*/m = 1.2$ to 1.5. The magnitude and approximate isotropy again indicate they pertain to h_7.

VIII. LONGITUDINAL-FIELD RESONANCES

With $\mathbf{H} \| \mathbf{q}$ well-defined resonance absorption peaks, periodic in $1/H$, were obtained. The period is proportional to the sound frequency. These resonances can arise from a dimensional matching of the sound wavelength to a characteristic repeat distance in the carrier trajectory parallel to the applied field. The repeat distance is covered in the time interval $2\pi/\omega_c$. If, for a surface possessing an r-fold symmetry axis parallel to $\mathbf{H}$, $\bar{V}_H$ is the average velocity along $\mathbf{H}$, then the condition for dimensional resonance can be written

$$|\bar{V}_H| 2\pi/\omega_c = (nr \pm \omega/\omega_c)\lambda, \quad \text{for } n \text{ an integer.} \quad (4)$$

The term $\omega\lambda/\omega_c$ accounts for the finite wave velocity. Using the relation $|\bar{V}_H| = \hbar/2\pi m^* |\partial A/\partial k_z|$ we obtain for the period,

$$\Delta(1/H) = \frac{e\lambda r}{c\hbar |\partial A/\partial k_z| (1 \mp V_S/\bar{V}_H)}. \quad (5)$$

Equation (4) is also the condition for Doppler-shifted cyclotron resonance.[21] The periodic attenuation peaks obtained with $\mathbf{q} \cdot \mathbf{H} \neq 0$ have been interpreted in terms of both the temporal[22] and dimensional resonances.[23] The period of the oscillations (in both cases) is determined by those k-space orbits for which the real space distance along the field direction covered in a cyclotron period is stationary in k_z, i.e., $\partial^2 A/\partial k_z^2 = 0$. For a convex surface where this condition does not occur, Eckstein[22] finds the period to be determined by $\partial A/\partial k_z$ at the elliptic limiting point (where $\mathbf{H}$ is normal to the Fermi surface). Quinn[24] has also shown that for $\mathbf{q} \| \mathbf{H}$ dimensional resonances with the longitudinal extent of (real space) tilted closed orbits can occur. However, this behavior gives rise to sinusoidal[25] rather than resonant-type acoustic absorption. Kaner *et al.*[15] also calculate periodic sound absorption for $\mathbf{q} \cdot \mathbf{H} \neq 0$. Their period [in Eq. (5)] is determined by those orbits for which $\mathbf{q} \cdot \bar{V}_H = 0$ at one point only, i.e., real space orbits which are parallel to the sound-wave front at one point only during a cyclotron period. Based on the calculated Fermi surface, no such orbits occur for $\mathbf{q} \| [0001]$.[26]

TABLE II. Longitudinal-field resonances.

H Units	ν (Mc/sec)	$\Delta(1/H)$ (10^{-5} G^{-1})	$\frac{1}{r}\left\|\frac{\partial A}{\partial k_z}\right\|$ (10^8 cm^{-1})	$\frac{\bar{V}_H m^*}{r\ m}$ (10^7 cm/sec)
[0001]	930	5.72	1.66	3.06
[0001]	930	36.8	0.258	0.475
[10$\bar{1}$0]	530	11.6	1.37	2.52

In Table II we give the observed periods for the longitudinal-field resonances and the related values of $(1/r)|\partial A/\partial k_z|$ and $\bar{V}_H m^*/rm$. In Table III are given the $(1/r)|\partial A/\partial k_z|$ at the elliptic limiting points of h_5 and h_7 calculated from the Fermi surface of Mattheiss. (Calculations for h_7 were made by approximating this piece by an ellipsoid.) For h_6 no reliable estimates could be made. With $\mathbf{H} \| [0001]$ there are two e_8 orbits where

TABLE III. Extremal and elliptic limiting point (ELP) values of $\partial A/\partial k_z$.

H	Fermi sheet	r[a]	$\frac{\partial^2 A}{\partial k_z^2}$	k_z	$\frac{1}{r}\left\|\frac{\partial A}{\partial k_z}\right\|$ (10^8 cm^{-1})
[0001]	h_5	2	···	*ELP*	1.18
[0001]	h_7	2	···	*ELP*	1.65
[0001]	e_8 cavity	1	···	*ELP*	0.57
[0001]	e_8	6	0	$(1/8)\bar{\Gamma}\bar{A}$	0.28
[0001]	e_8	6	0	$(14/15)\bar{\Gamma}\bar{A}$	1.66
[10$\bar{1}$0]	e_8 cavity	2	···	*ELP*	0.5
[10$\bar{1}$0]	h_5	2	···	*ELP*	0.033
[11$\bar{2}$0]	h_5	2	···	*ELP*	0.40
[11$\bar{2}$0]	h_7	2	···	*ELP*	1.20

[a] r gives the order of the rotational symmetry.

[21] T. Kjeldaas, Jr., Phys. Rev. **113**, 1473 (1959).
[22] S. G. Eckstein, Phys. Letters **20**, 144 (1966).
[23] B. K. Jones, Phil. Mag. **9**, 217 (1964).
[24] J. J. Quinn, Phys. Rev. Letters **7**, 316 (1963).
[25] O. Beckman, L. Ericksson, and S. Hörnfeldt, Solid State Commun. **2**, 7 (1964).
[26] A possible exception may exist for the noncentral extremal area orbit ($\mathbf{H} \| [0001]$) of h_6 which can have a longitudinal projection in real space. The physical situation is similar to that calculated by Quinn. No accurate values of the Fermi velocities for this orbit can be obtained from the calculations of Mattheiss.

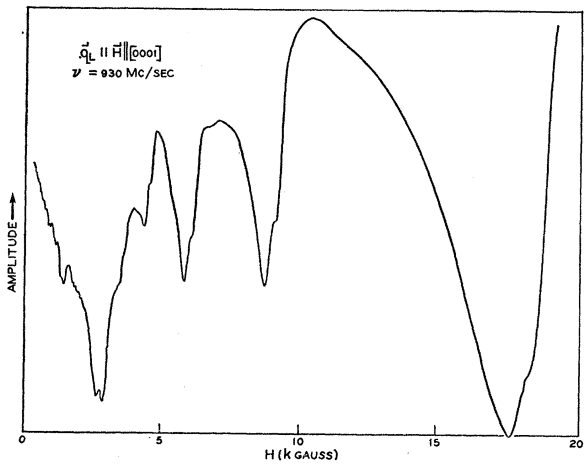

FIG. 13. Echo amplitude versus magnetic field for $\mathbf{q}\|\mathbf{H}\|[0001]$, and $\nu=930$ Mc/sec.

$\partial^2A/\partial k_z^2=0$. These occur at approximately 1/8 and 14/15 the ΓA distance from Γ (see Fig. 1). The values of $(1/r)|\partial A/\partial k_z|$ for these orbits are also given in Table III. For the orbit closer to Γ, the values are probably an inaccurate description of the actual Fermi surface, since the calculated curvature has not been observed in the dH-vA and magnetoacoustic dimensional-resonance experiments. Accurate calculations for orbits with $\partial^2A/\partial k_z^2=0$ on h_6 and (possibly) h_7 cannot be made.

With $\mathbf{H}\|[0001]$ the observed period $\Delta(1/H)=5.72\times10^{-5}$ G^{-1} is in good agreement with that calculated for both the elliptic limiting point of h_7 ($r=2$) and for orbits with extremal $\partial A/\partial k_z$ on e_8 ($r=6$). The remaining period $\Delta(1/H)=36.8\times10^{-5}$ G^{-1} is probably associated with h_6 or e_8. (Although rough agreement is obtained with the e_8 orbit having the smaller extremal $|\partial A/\partial k_z|$, the calculated value, as mentioned above, is probably inaccurate.) For this period the fundamental absorption peak (see Fig. 13) is split by about 115 G. Such a splitting can result from the differences in resonances for electrons traveling with and those traveling against the sound wave [cf. the term $(1\mp V_S/\bar{V}_H)$ in Eq. (5)]. The fractional splitting is given by $2V_S/\bar{V}_H$. The observed splitting yields $(1/r)m^*/m=0.175\pm0.025$ and $\bar{V}_H=2.76\pm0.4\times10^7$ cm/sec.

For $\mathbf{H}\|[10\bar{1}0]$ the observed period is $\Delta(1/H)=11.6\times10^{-5}$ G^{-1}. The limiting point values of $\partial A/\partial k_z$ for the h_5 pieces are too small to give this period. For the 60° rotated pieces of h_7 ($r=1$) the limiting point $\partial A/\partial k_z$ will not be very different from the value calculated along $[11\bar{2}0]$. This value is too large to yield the experimental result. For the h_7 sheets which have a twofold symmetry axis parallel to $[10\bar{1}0]$ there is an elliptic limiting point (ELP) at the point of degeneracy with e_8. Since the h_7 Fermi-surface contour in the ALM plane is not orthogonal to the AL line at this point, $\partial A/\partial k_z=0$. Another ELP on h_7 occurs with $\mathbf{H}\|[10\bar{1}0]$ but the calculated shape at this point is not accurate. The observed value, therefore, probably pertains to h_6 or e_9.

IX. CONCLUSIONS

To a considerable extent the results of the magnetoacoustic studies have complemented the dH-vA work. Our data have generally clarified the shape of the larger pieces of the Fermi surface while for the smaller pieces a more detailed description has been provided by the dH-vA work. The evidence, from our studies, supporting the presence of the e_8 cavity is reasonably consistent with the dH-vA data. Over an angular range of 20°, however, the shape is not well established, leaving some of the dH-vA behavior unexplained.

Except for some minor repairs, the Fermi surface calculated by Mattheiss is in good agreement with extremal areas and caliper dimensions obtained by experiment. Effective masses and velocities, obtained from the calculations, are considerably less reliable than the extremal dimensions, and a confrontation of these numbers with the relevant magnetoacoustic data is not always possible. It has been possible to make plausible assignments of some of the mass-velocity data (from the longitudinal-field resonances) to specific orbits on one or two sheets of the Fermi surface from the APW calculations. For the remaining data the relevant piece of the Fermi surface is surmised by a reasonable exclusion of all others. Much of the uncertainty here is due to ignorance of the 9th-zone electron sheet—if it exists.

ACKNOWLEDGMENTS

The authors express their gratitude to V. G. Chirba and H. V. Dail for technical assistance, and to L. F. Mattheiss, A. S. Joseph, and A. C. Thorsen for helpful discussion.